Combined Blast & Fragment Test for Textiles: Effect of the stochastic response of electrical detonators on the time interval between consecutive loads

T. Gerlache[1], G. Kechagiadakis[1] and D. Lecompte[1]

[1] *Royal Military Academy, Avenue de la Renaissance 30, 1000, Brussels, Belgium*

Abstract. Protective textiles for military applications must withstand both fragment and blast impacts. However, current testing protocols solely assess ballistic resistance, overlooking the complex dynamic interactions between blast waves and high-velocity fragments. This results in an inadequate evaluation of protective performance for real-world explosive scenarios. To address this, an experimental setup capable of generating a synchronized planar blast wave and high velocity fragment is used to evaluate the explosion resistance of various textile solutions. A key challenge of the setup lies in precisely controlling the time interval between blast and fragment impacts, as the resistance of the textiles varies depending on the impact phase. At critical time intervals, textiles exhibit reduced impact resistance. The primary source of uncertainty in this timing control stems from variability in the detonator's response time after receiving the initiation signal. To quantify and refine control over this delay, two electrical circuits are designed: one employing a voltage divider to measure the response time and one integrating a custom-made shunt to monitor the current flowing through the detonator prior to detonation. Tests are conducted under various laboratory power supply conditions (20V/2.5A, 30V/2.5A, 60V/2.5A) and utilizing a blast machine to characterize the detonator's response across different operating configurations. By accurately characterizing the detonator's initiation parameters, including timing precision and energy input, a predictive rough estimation of the detonation time delay can be developed in function of the voltage input. The results will guide the development of the next generation of protective textiles.

1. INTRODUCTION

Protective textiles used in military applications have to withstand both fragment and blast impacts. In real-world scenarios, such as encounters with grenades or improvised explosive devices, these materials are subjected to a combination of high-velocity fragments and intense pressure waves. The interaction between these two loading conditions is complex and can significantly alter the textile's protective performance. A key factor influencing this response is the timing between the blast wave and the fragment impact. Depending on several factors such as the phase of the textile's oscillation at the moment of impact, the interaction can either enhance energy absorption or reduce penetration resistance 0. In certain cases, this coupled effect results in greater damage than the sum of both loads applied independently. Despite this known phenomenon and the ability of fabrics to reflect and absorb blast waves depending on material and structural properties such as internal damping, layer sequencing, and density, protective materials are still solely evaluated based on ballistic resistance, neglecting the potential vulnerabilities introduced by combined loading conditions.

As found in 0, the time interval between the two loading events is a critical factor influencing textile performance. The blast wave induces oscillations that alter key parameters such as relative impact velocity and the fabric's stress state, affecting its resistance to penetration. This interaction occurs within a narrow timeframe of approximately a few hundred microseconds. Therefore, to systematically investigate different loading configurations—including blast-first versus fragment-first impacts and varying time delays—microsecond control over the time interval between the two loads impacting the textile is essential.

The primary source of uncertainty in timing control arises from variations in the electrical detonator's response time after receiving the initiation signal. This response is inherently inconsistent, exhibiting fluctuations of more than 125 microseconds compared to the intended detonation time for the used 30V/2.5A laboratory power supply, making precise microsecond-level control in a combined loading setup unfeasible.

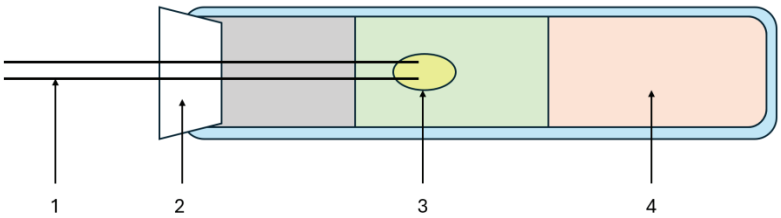

Figure 1. Schematic overview of electrical detonator components

https://doi.org/10.52202/081621-0050

As shown in Figure 1, the electrical detonator consists of four main components. When an electrical voltage is applied across the detonator wires (1), energy is supplied to ignite the primary explosive (3), which in turn initiates the detonation of the secondary explosive (4). A closing tip (2) is used to shield the internal components from external influences.

Variations in detonation time primarily arise from two factors: the electrical power supplied to the detonator and inconsistencies in the masses of the primary and secondary explosives. This paper focuses on investigating the influence of the first factor. While manufacturers specify the minimum energy required for detonation through a recommended input voltage, this information provides little insight into how variations in input voltage influence the speed of the detonation process. A higher input power is expected to shorten detonation time, yet its influence on timing variability has not been stochastically described.

This study aims to characterize the detonation time and variations to changes in input power. This by examining the stochastic behaviour of in-field used electrical detonators under various power supply configurations. In total, 45 detonators are tested experimentally using the same power supply available in the laboratory for the following configurations: 20V/2.5A, 30V/2.5A, and 60V/2.5A. This provides an overview of the influence of lowering and raising the supplied voltage compared to the currently used 30V/2.5A. The current is limited to 2.5A, which is maximal for the used power supply. Furthermore, 13 experiments are conducted using a blast machine, as shown in Figure 2. This device is employed in military applications for initiating electrical detonators and is able to generate high voltages compared to the available laboratory power supplies.

Figure 2. Blast machine used in military applications

The results of the experiments highlight the current level of control and offer insight into how further improvements could enhance synchronization and reliability in combined loading scenarios.

https://doi.org/10.52202/081621-0050

2. METHODS

To characterize detonation time and its variations in function of the power supply, a series of experiments was designed. Each test measures the detonation time delay (Δt), defined as the time interval between the activation signal received by the detonator ($= t_{begin}$) and the detonation of the primary explosive ($= t_{end}$). A custom-built electrical circuit, illustrated in Figure 3, was implemented to capture both moments in time and is used for each experiment for the four power supply configurations.

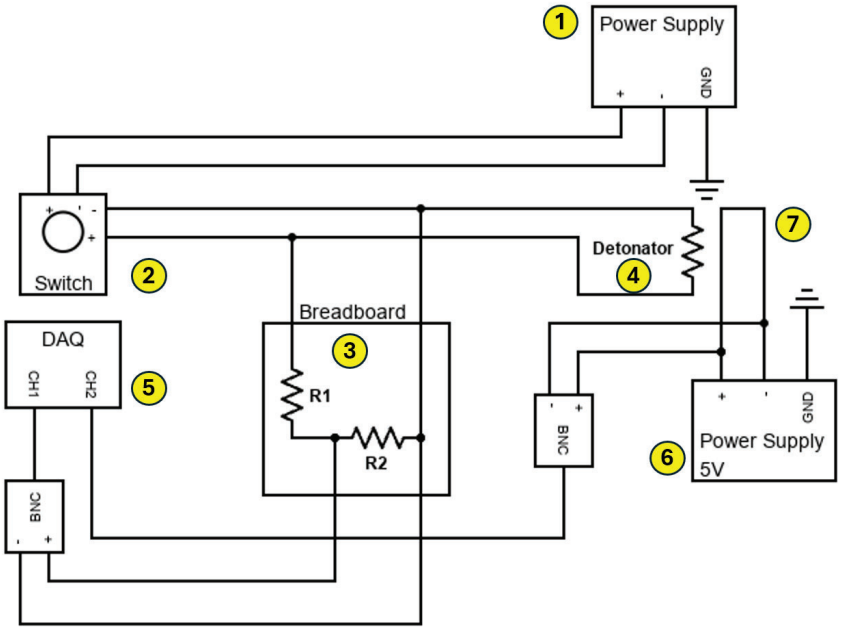

Figure 3. Custom-built electrical circuit for activation- and detonation signal detection

The switch (2) serves as the activation signal by connecting the power supply (1) to the detonator (4), initiating current flow and defining the measurement start point ($= t_{begin}$). A voltage divider, connected in parallel with the detonator via a breadboard (3) is used to capture this moment in time. This by measuring the voltage across the second resistor (R_2), referred to as the 'R_2 voltage'. The voltage divider was made using laboratory-available resistors, selected to keep the measuring voltages below the 10V limit of the data acquisition system (DAQ). Given the known ratio between R_1 and R_2, the actual power supply voltage over time can be deducted using Equation 1.

For all power supply configurations, except for the blast machine, the voltage divider is implemented with resistor values $R_1 = 99.7k\Omega$ and $R_2 = 4.661k\Omega$. This results in an output voltage below 3V for a 60V power supply input. Since the exact voltage output of the blast machine is unknown, the voltage divider is configured to remain below the DAQ safety limit for kilovolt-level inputs with $R_1 = 1.005M\Omega$ and $R_2 = 330.3\Omega$.

$$V_{source} = V_{R_2} \cdot \frac{R_2}{R_1} \tag{1}$$

To detect the explosion of the primary explosion, a separate wire (7) connected to a 5V power supply (6) is taped onto the detonator, with its signal recorded by the DAQ (5) as the 'Taped wire voltage'. Upon detonation, the explosive force severs the wire, causing a change in the measured electrical signal, which is registered by the DAQ. This break in continuity marks the detonation event of the primary explosive ($= t_{end}$), and in combination with the trigger voltage, allows for the measurement of the detonation time delay (Δt).

An example of a detonation time delay measurement for the 20V/2.5A configuration is presented in Figure 4. The start- and end times are indicated with black crosses, with the duration in between corresponding to the detonation time delay. At the beginning of the measurement, a voltage peak is observed, followed by a non-smooth fluctuation before stabilizing. This behaviour is attributed to internal impedance of the power supply and ends with the activation of the current limit, resulting in a peak. Next, the current stabilizes until detonation of the primary explosive occurs, with an intermediate peak reflecting the moment where the current limit is reached.

https://doi.org/10.52202/081621-0050

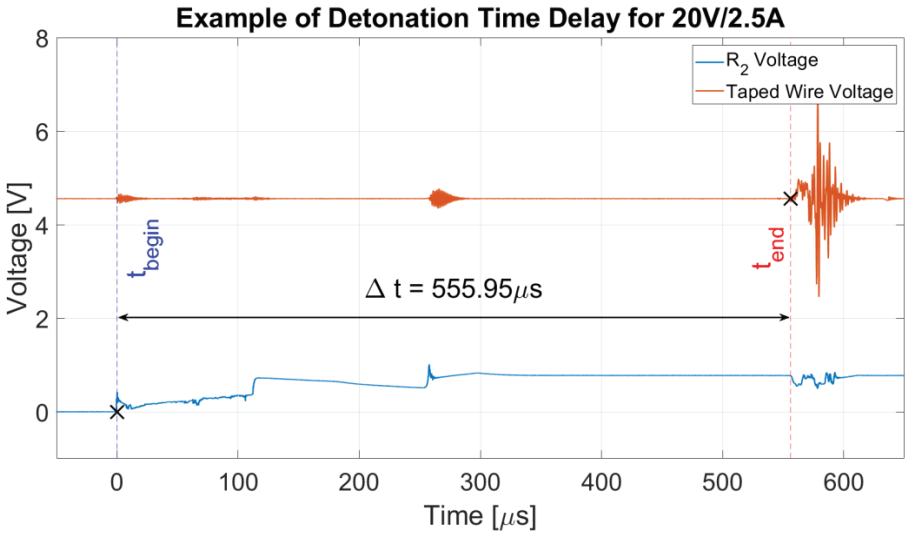

Figure 4. Example of detonation time delay deduction for 20V/2.5A power supply

The energy dissipation with the laboratory power supply is discussed in section 4.2, where a shunt resistor is placed in series with the detonator to measure the current flowing through the detonator. Additionally, interference between the 'R_2 voltage' and the 'Taped wire voltage' is observed, originating from the DAQ itself. The influence of this interference does not interfere with the accuracy of the measurements.

In total, 45 detonators are tested experimentally for each of the three laboratory power supply configurations: 20V/2.5A, 30V/2.5A, and 60V/2.5A. Additionally, 13 experiments are conducted using a blast machine. For each test, the applied power supply voltage is recorded, and the detonator resistance is measured. Additionally, it is noted if a detonator is taken from a different pack. This to have an overview on the influence of the batch on the detonation time. Data acquisition is performed at a 20MHz sample rate, and the detonation time delay is determined from the resulting measurement plots.

https://doi.org/10.52202/081621-0050

3. RESULTS

This section gives an overview of the results, given in Table 1. These outcomes together with the corresponding sample mean $\bar{x}$ and sample standard deviation s are shown in Figure 5.

Table 1. Experimental results for 20V/2.5A, 30V/2.5A, 60V/2.5A, and blast machine power supplies

20V/2.5A Total of 15 experiments			
Voltage [V]	$R_{detonator}$ [Ω]	Δt [µs]	Pack
20.3	2.8	555.95	1
20.4	2.8	513.95	1
20.4	2.8	475.05	1
20.4	2.7	475.40	1
20.3	2.7	456.50	1
20.2	2.7	597.70	2
20.2	2.7	532.00	2
20.2	2.7	551.40	2
20.2	2.8	526.90	2
20.1	2.7	481.70	2
20.2	2.7	446.85	2
20.1	2.7	465.05	2
20.1	2.7	568.70	2
20.2	2.7	521.60	2
20.1	2.7	514.45	2

30V/2.5A Total of 14 experiments			
Voltage [V]	$R_{detonator}$ [Ω]	Δt [µs]	Pack
30.2	2.7	554.30	1
30.4	2.7	364.45	1
30.4	2.7	408.90	1
30.4	2.6	361.40	1
30.4	2.7	352.45	1
30.5	2.9	326.75	1
30.4	2.6	410.00	1
30.4	2.6	401.20	1
30.4	2.6	441.80	1
30.4	2.6	544.75	1
30.3	2.7	447.80	2
30.4	2.7	329.50	2
30.4	2.6	414.05	2
30.4	2.6	382.70	2

60V/2.5A Total of 16 experiments			
Voltage [V]	$R_{detonator}$ [Ω]	Δt [µs]	Pack
60.5	2.7	261.05	1
60.7	2.8	231.60	1
60.7	2.7	275.70	1
60.7	2.6	350.70	1
60.5	2.5	251.70	1
60.6	2.8	272.95	1
59.9	2.8	270.85	2
59.9	2.7	289.00	2
60.0	2.6	324.05	2
60.0	2.6	268.80	2
60.0	2.8	336.15	2
60.0	2.6	384.15	3
60.0	2.6	313.70	3
60.0	2.7	260.00	3
60.0	2.7	301.70	3
60.0	2.7	265.20	3

Blast Machine Total of 13 experiments			
Voltage [kV]	$R_{detonator}$ [Ω]	Δt [µs]	Pack
27.4	2.6	106.50	1
27.2	2.6	98.65	1
25.7	2.6	108.00	1
25.3	2.7	102.30	1
27.1	2.6	94.25	1
25.9	2.5	82.75	1
26.7	2.5	104.90	1
27.8	2.6	92.70	1
28.9	2.6	72.55	1
25.0	2.9	117.45	2
26.1	2.6	119.65	2
25.1	2.7	86.45	2
24.7	2.7	89.35	2

https://doi.org/10.52202/081621-0050

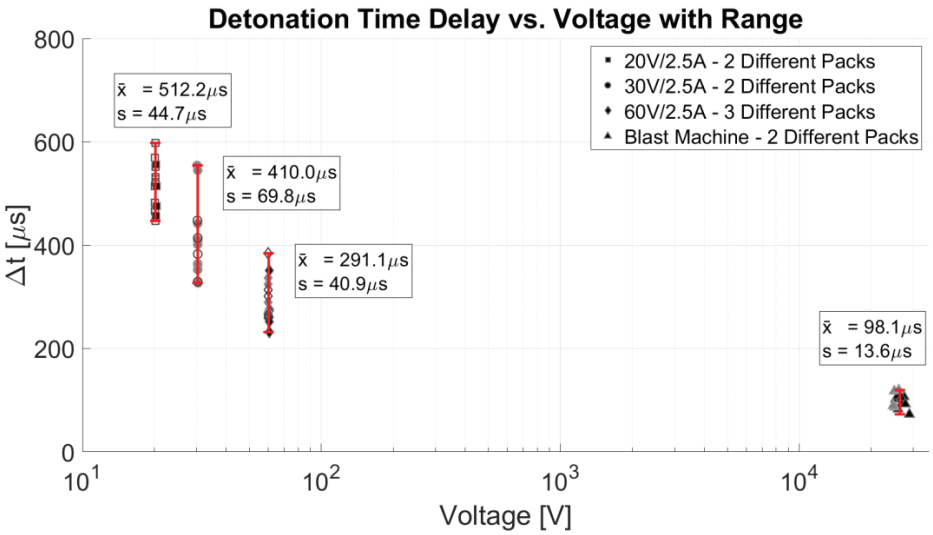

Figure 5. Graphical overview of the experimental results with sample mean and sample standard deviation indicated

4. DISCUSSION

This section discusses the results by describing the statistical distribution of the detonators as a population, after which the energy dissipation using the laboratory power supplies is detailed. Finally, an overview of the blast machine is discussed and a predictive rough estimation graph can be setup.

4.1 Normal distribution

Given the small sample sizes, it is necessary to describe the statistical distribution of the detonator population as a whole. The probability plot shows for each dataset that the population follows a normal distribution. This conclusion is further supported by p-values well above 0.05 for each power supply configuration. Consequently, t-statistics can be applied to estimate the confidence intervals for each configuration.

The confidence interval of the population mean (μ) can be calculated using t-statistics using Equation 2. For a 95% confidence interval, α is set to 0.05. With corresponding t-statistic, $t_{\alpha/2}$ is obtained from standard statistical tables, with n representing the sample size and s the sample variance, which determines the standard error of the mean $\sigma_{\bar{x}}$. These values, along with $\bar{x}$, are illustrated in Figure 5.

$$\mu = \bar{x} \pm \left(t_{\alpha/2}\right) \sigma_{\bar{x}} = \bar{x} \pm \left(t_{\alpha/2}\right) \frac{\sigma}{\sqrt{n}} \approx \bar{x} \pm \left(t_{\alpha/2}\right) \frac{s}{\sqrt{n}} \tag{2}$$

Similarly for the population variance, confidence interval is calculated using Formula, where the χ^2 obtained from standard statistical tables as well using Equation 3.

$$\frac{(n-1)s^2}{{\chi^2}_{\alpha/2}} \leq \sigma^2 \leq \frac{(n-1)s^2}{{\chi^2}_{1-\alpha/2}} \tag{3}$$

The results for the four different power supplies are given in Table 2 and the best- and worst-case scenarios for the standard deviation control for a 95% ($= 2\sigma$) certainty are listed in Table 3.

Table 2. 95% certainty intervals of the population mean and standard deviation for each power supply

Population 95% Certainty Intervals	μ [μs]	σ [μs]
20V	512.2 ± 24.7	$32.7 \leq \sigma \leq 70.4$
30V	410.0 ± 40.3	$50.6 \leq \sigma \leq 112.5$
60V	291.1 ± 21.8	$30.2 \leq \sigma \leq 63.3$
Blast Machine	98.1 ± 8.2	$9.7 \leq \sigma \leq 22.4$

Table 3. Best- and worst-case 2σ intervals for each power supply

95% certainty ($= 2\sigma$)	Best-case [µs]	Worse-case [µs]
20V	65.4	140.8
30V	101.3	225.1
60V	60.4	126.5
Blast Machine	19.4	44.9

4.2 Laboratory Power Supply

A decrease in the confidence interval for the population mean and standard deviation is present between 20V and 60V. The results of 30V do not follow this same trend as two measurements leading to a noticeable deviation, as shown in Figure 5. One of the causes of this discrepancy is thought to be a difference in the amount of primary explosive in the detonator itself, needing more energy to initiate the explosion. These two extremes come from detonators of the same pack. Hence, an argument can be made to investigate the differences in detonation time caused by the discrepancies in amount of explosives present in the detonator. However, too few experiments were conducted to make a conclusion regarding the batch influence. Nonetheless, the overall trend of the population statistics getting more controllable going from 20V/2.5A to 60V/2.5A is still present. While the improvement of the 95% certainty interval with a 40V is present, it remains relatively limited as listed in Table 3. Nonetheless, it shows the influence of the input voltage which can be understood by analysing the energy dissipation of the detonator using the power supply.

The energy distribution is determined from the current flowing through the detonator, measured using a shunt. A custom shunt was created using a simple wire, which was relatively long, introducing inductance into the measurement. This electrical component was placed in series with the detonator and the voltage divider was removed to minimize interference of other components. As a consequence of the increased inductance due to the shunt, the detonation time delay is slightly extended, making it an imperfect representation of the detonation time itself. However, it still provides an overview of the energy dissipation relative to the detonation time and is shown in Figure 6. The power supplied to the detonator is calculated using Equation 4, and integrating it over time yields the dissipated energy.

$$P = I^2 \cdot R_{detonator} \tag{4}$$

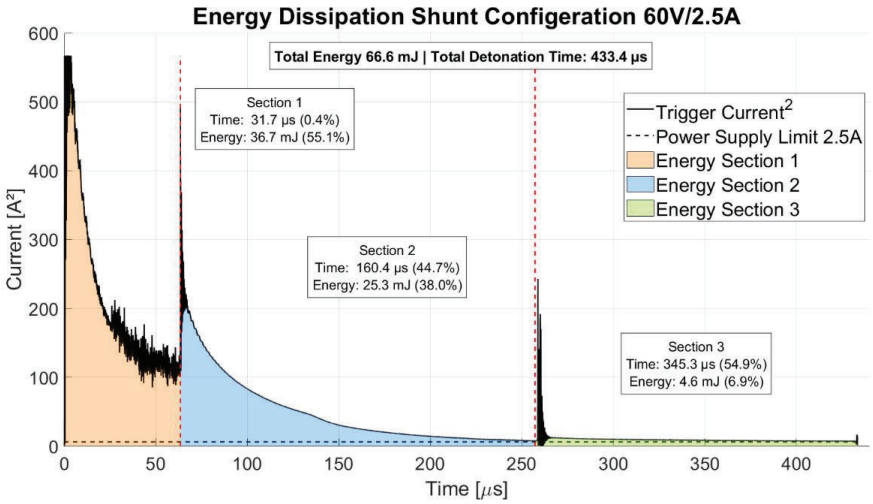

Figure 6. Energy dissipation of detonator measured using shunt configuration with 60V/2.5A power supply

https://doi.org/10.52202/081621-0050

The energy dissipation process can be categorized into three distinct sections. The first phase corresponds to the period before the activation of the power supply's current limit control loop. During this phase, the current reaches the theoretical short-circuit value, leading to a high power output dissipated by the detonator. As shown in Figure 6, over 55% of the total power is delivered to the detonator in less than 0.5% of the total detonation time delay. A gradual decline in power is observed in this phase due to the internal impedance of the power supply. Section 1 concludes with the activation of the current limiting circuit, resulting in a characteristic peak. The transition between the first- and second phases is not consistent, exhibiting variations of up to 100 µs and will differ from power supply to power supply.

The second phase is characterized by a gradual exponential decrease in current, regulated by the current limiting circuit, which reduces the voltage to maintain the current within the specified limit. During this phase, approximately 38% of the total power is dissipated over a proportion of about 44% of the detonation time delay. The end of this phase is marked by the power supply's control loop recognizing that the current has fallen below the maximum threshold of 2.5A. Consequently, the voltage is no longer reduced, leading to the deactivation of the voltage-limiting circuit. This transition may result in a secondary peak, as observed in Figure 6.

The third section is characterized by a relatively small energy output over a big proportion of the detonation time delay. It would be expected that a higher maximum current would result in a higher energy output in the second but mostly in the third section, leading to a lower detonation time delay. To investigate this effect, additional experiments were conducted using 40V/30A and 30V/5A configurations. However, the results remained within the same order of magnitude, showing no significant improvement.

It is concluded that the first phase is the most crucial in energy delivery, as it corresponds to the short-circuit current condition, where a substantial amount of energy is transferred within a very short time interval. This first section is constrained by the capabilities of laboratory-grade power supplies, indicating that the power source required for precise microsecond control of the detonation time delay is external, such as the use of a blast machine.

4.3 Blast Machine

Unlike laboratory power supplies, the blast machine is not restricted by current-limiting mechanisms and is capable of delivering a high energy peak over a short duration. As a result, it is particularly effective in the initial phase of energy delivery, as shown in Figure 6.

Figure 7 depicts a simplified version of the electrical circuit of a blast machine. These devices use a small single-phase alternator (1), which is mechanically driven by a handle-actuated plunger. The electrical output from the alternator is rectified (2) and subsequently stored in one or more capacitors (3). Once sufficient energy has been accumulated, the Zener diode allows current to flow and an LED indicator (4) lights up, signalling that the system is ready to discharge. By pressing the switch (5), the circuit releases the stored energy to the output terminals, where the detonator (6) is connected. Additional resistors are incorporated to safeguard circuit components. In the absence of a connected blasting circuit such as a detonator, the stored energy is dissipated through an internal bypass circuit, which is not included in the schematic representation in Figure 7.

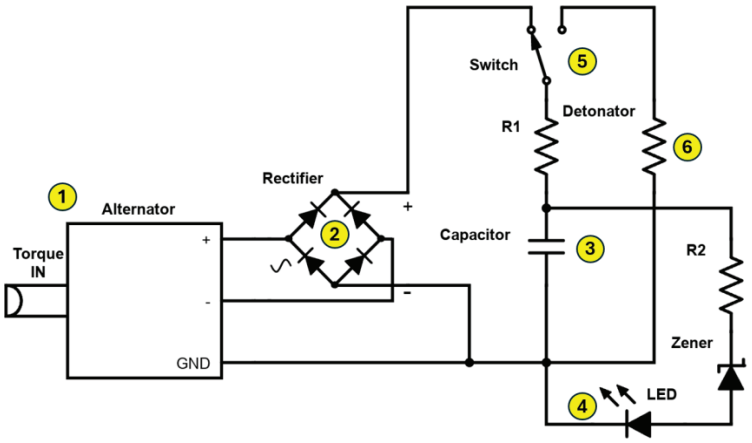

Figure 7. Simplified schematic overview of blast machine electrical circuit

The voltage output of the blast machine reaches a peak of approximately 25 kV. Even after the initial peaks start to settle, the voltage remains at approximately 350V between 20 µs and 40 µs, as illustrated in Figure 8.

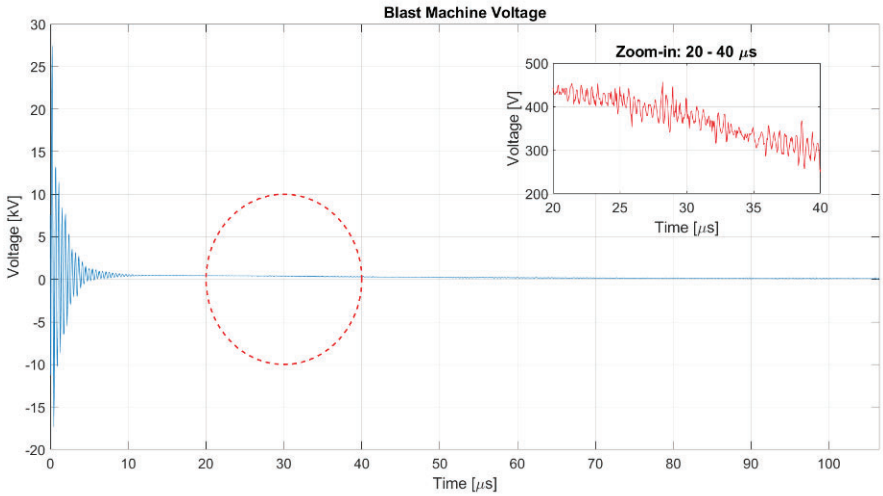

Figure 8. Blast machine voltage with 20-40µs zoom

The capacitor discharge principle significantly increases the energy supplied to the detonator upon the moment of pressing the trigger switch, reducing the mean detonation time delay by a factor of more than five and its standard deviation by a factor of more than three as listed in Table 3. Consequently, it is concluded that a kilovolt-range peak voltage is needed for microsecond level control between consecutive blasts and fragment impacts of which a blast machine is an effective example.

4.4 Predictive Rough Estimation

With increasing voltages, the control in detonation time delay increases. This trend is visible in Figure 5 and allows to fit a logarithmic predictive curve through the obtained datapoints and estimate the change in control with further increasing the supplied voltage. Given the normal distribution of the data, the sample standard deviation can be estimated using Equation 5. This enables the formulation of predictive rough estimates for the expected outcome of increasing the peak voltage, as illustrated in Figure 9.

$$\sigma_{\bar{x}} = \frac{Range}{4} \tag{5}$$

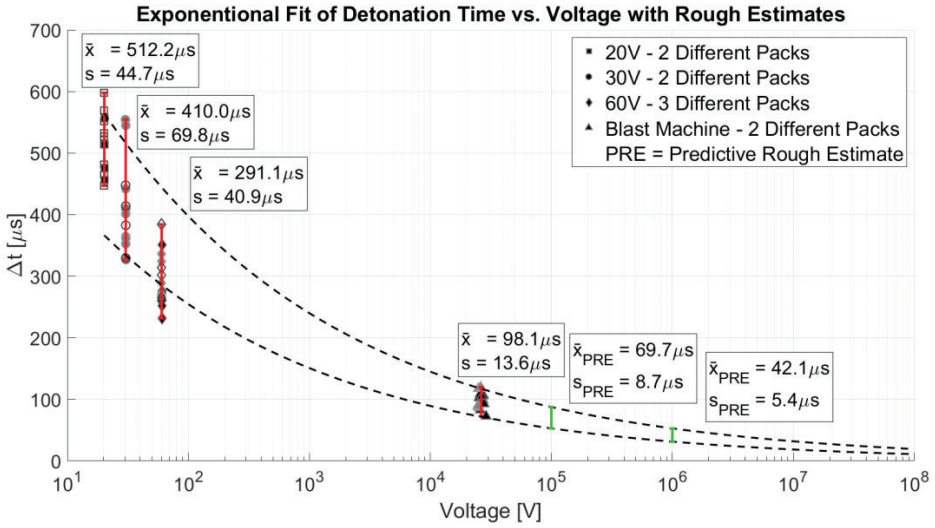

Figure 9. Exponential fit of detonation time vs. voltage with rough estimates

https://doi.org/10.52202/081621-0050

The exponential fit predicts that increasing the input voltage from 25 kV to 1000 kV results in a reduction of both the sample mean and sample standard deviation by more than a factor of two. While this remains a rough estimate, it demonstrates that the level of control over detonation timing can be improved for the tested detonators.

However, practical implementation of capacitor discharge circuits of the range of 1000 kV is challenging. Additionally, the achievable control remains within the microsecond range. Reducing this further to the scale of a few hundred nanoseconds is not considered realistic with the tested in-field used detonators, as these are not designed for such high precision. Therefore, the use of specialized detonators tailored for this level of accuracy should be explored.

5. CONCLUSION

The influence of input voltage on the variability of the detonator response time was experimentally investigated by characterizing the detonation time delay across different configurations using a laboratory power supply. Results showed that increasing the voltage generally improved timing control, with the mean detonation time decreasing from 512.2µs at 20V/2.5A to 291.1µs at 60V/2.5A. However, the reduction in variability was limited, as the worst-case standard deviation (with 95% certainty) only improved from 140.8µs to 126.5µs. These advancements remain constrained by the inherent limitations in laboratory power supplies. To overcome these limits, a capacitor discharge system from a blast machine was tested, achieving peak input voltages of 25 kV. A reduction of the mean detonation time delay to 98.1µs and the worst-case standard deviation to 44.9µs was observed, showing noticeable improvements. This enabled the development of a predictive rough estimation graph of the performance at even higher voltages, showing further increase in controllability with increasing input voltage.

However, achieving microsecond-level precision, which is desired for controlling the synchronized loading of textiles, remains complex. This is due to the difficulties of integrating high-voltage capacitor discharge systems into existing setups and the inherent batch-to-batch variability of in-field-used detonators. Addressing these challenges may require a combination of an optimized capacitor discharge firing system together with dedicated high-precision detonators.

Acknowledgements

I would like to thank **Maxym Desauvage** for his support during the experiments and for his valuable contributions to the discussion of this study.

References

[1] Kechagiadakis, G., Lecompte, D., Van Paepegem, W., Coghe, F., and Pirlot, M.. International Journal of Impact Engineering, 185 (2024), 104830.